Nuclear Science and Techniques (2026) 37:106
https://doi.org/10.1007/s41365-026-01933-2

Single-reference $B\rho$-defined isochronous mass spectrometry for mass measurements of exotic nuclei

Yin-Fang Luo[1,2] · Jia-Hao Lv[1,2] · Yuan-Ming Xing[1,2] · Min Zhang[1] · Yu-Hu Zhang[1,2] · Meng Wang[1,2] · Yury A. Litvinov[1,3] · Xiao-Hong Zhou[1,2]

Received: 6 May 2025 / Revised: 11 August 2025 / Accepted: 18 August 2025 / Published online: 26 March 2026

Abstract
$B\rho$-defined isochronous mass spectrometry ($B\rho$-IMS), established at a storage ring, is a valuable tool for determining the masses of short-lived nuclei. In previous $B\rho$-IMS experiments, the effects of magnetic field drifts had to be corrected to improve the mass resolving power of $B\rho$-IMS [Eur. Phys. J. A 59, 27 (2023)]. The correction procedures are complicated and require multiple reference ions with well-known masses in each injection, which may not be the case in the measurements of exotic nuclei with tiny production yields. In this study, we propose a novel approach to $B\rho$-IMS that requires only single reference ion for mass determination in an individual injection, avoiding tedious and complicated correction procedures. This approach achieves mass precision comparable to that of previous $B\rho$-IMS results and is proven to be suitable for future mass measurements of exotic nuclei with extremely low production yields.

Keywords Storage ring · $B\rho$-defined isochronous mass spectrometry · Double time-of-flight (TOF) detectors · Nucleus mass measurement

1 Introduction

Mass spectrometry of nuclei or ions has wide applications in nuclear physics [1] and other areas [2, 3]. Isochronous mass spectrometry (IMS) conducted at the Cooler Storage Ring for experiments (CSRe) in Lanzhou, China, has emerged as a pivotal technology for nuclear mass determination. This method has yielded numerous new mass values [4–10], demonstrating itself as an essential tool in nuclear mass spectrometry [11–13].

Early IMS experiments relied on the measurements of revolution times (T) of stored ions, and high resolving power was achieved only for the ion species of limited mass-to-charge ratios (m/q), fulfilling the so-called isochronous condition of $\gamma = \gamma_t$ [14]. Here, γ is the relativistic Lorentz factor of the ion, and γ_t is the transition point, which is an ion-optical quantity of the ring. However, for the majority of ion species with $\gamma \neq \gamma_t$, the time resolutions inevitably deteriorate depending on how far the γ's differ from γ_t [15].

To make the IMS broadband, great efforts have been made [16, 17], and an additional velocity (v) measurement at the straight part of the ring has also been proposed [15, 18]. Velocity measurements were finally realized at the CSRe [19, 20], which allowed for the determination of both the orbit length, $C = vT$, and magnetic rigidity, $B\rho = m/q\gamma v$, for reference ions with well-known masses. Consequently, the universal calibration function, $B\rho(C)$, is constructed, enabling the $B\rho$ determination for non-reference ions using their measured C values—thereby realizing the $B\rho$-defined IMS (or $B\rho$-IMS) [21, 22]. Using this technique, mass

This work was supported by the National Key R&D Program of China (No. 2023YFA1606401), the Youth Innovation Promotion Association of the Chinese Academy of Sciences (No. 2021419), the National Natural Science Foundation of China (Nos. 12135017, 12475128, 11961141004, and 12121005), and the CAS Project for Young Scientists in Basic Research (No. YSBR-002).

✉ Yuan-Ming Xing
xym@impcas.ac.cn

[1] State Key Laboratory of Heavy Ion Science and Technology, Institute of Modern Physics, Chinese Academy of Sciences, Lanzhou 730000, China

[2] School of Nuclear Science and Technology, University of Chinese Academy of Sciences, Beijing 100049, China

[3] GSI Helmholtzzentrum für Schwerionenforschung, Planckstraße 1, Darmstadt 64291, Germany

measurements with remarkable precision down to 5 keV have been achieved [23] and numerous new mass values have been determined for the first time [24–26]. However, to obtain an accurate $B\rho(C)$ function, one must eliminate the effect of magnetic field drifts during the experiment, which can be larger than $\sim 10^{-5}$. Thus, a complicated correction procedure has been developed, which requires multiple reference ions to correct for the change in the magnetic field for each injection [23]. This requirement is unfavorable for the mass measurement of exotic nuclei, as the number of reference ions in each injection can be quite low. Furthermore, the correction process may potentially introduce improper mass uncertainty assignments for both reference and non-reference ions (similar examples can be found in Ref. [27]).

To address these challenges, a new approach to $B\rho$-IMS is needed. Given the short storage time of ions in the ring (a few hundred microseconds) per injection, magnetic field drift becomes negligible over this short duration. Therefore, if the $B\rho$ value of non-reference ions can be directly determined via a single reference ion within the same injection, the need for correcting magnetic field drifts using multiple reference ions would be eliminated.

According to the definition of γ_t [14]:

$$\gamma_t^2 = \frac{\mathrm{d}(B\rho)/B\rho}{\mathrm{d}C/C}, \tag{1}$$

γ_t connects the $B\rho$ and C differences between two ions within the same injection, thereby enabling the $B\rho$ determination of a non-reference ion based on a single reference ion.

In this paper, we propose a novel method for $B\rho$-IMS that utilizes well-characterized γ_t values [28] for $B\rho$ and mass determination. This method demonstrates two key advantages: (1) It requires only a single reference ion per injection, and (2) it naturally reduces the effects of magnetic field drifts, thereby obviating the need for extra correction procedures. In Sect. 2, we outline the principle of this method. In Sect. 3, we exemplify its performance through an experiment [21, 23] using $^{58}Ni^{19+}$ as the primary beam. In Sect. 4, the Discussion is presented, followed by a summary and outlook in Sect. 5.

2 Principle of the new method

According to the fundamental equation $B\rho = \frac{m}{q}\gamma v$, the mass-to-charge ratio m/q of a stored ion can be expressed as:

$$\frac{m}{q} = B\rho \cdot \sqrt{\frac{1}{v^2} - \frac{1}{c^2}}, \tag{2}$$

where v is the velocity of the ion and c is the speed of light in vacuum. Because v is measured directly by the double time-of-flight (TOF) detectors installed in the straight section of the storage ring [20], the challenge in determining the unknown mass lies in the $B\rho$ determination.

In previous $B\rho$-IMS studies [21, 23], $B\rho$ and C were assumed to follow a $B\rho(C)$ curve characterized by an analytic function, which was used to determine the $B\rho$ values of non-reference ions based on their measured C values. However, the $B\rho(C)$ curve varies with time because of magnetic field drifts. To obtain an accurate $B\rho(C)$ function, a complicated method was utilized to mitigate the effect of the field drifts, as detailed in Ref. [23].

In this study, we propose a more straightforward approach to determine the $B\rho$ value of non-reference ions in each injection. For ions circulating in the ring, according to Eq. (1), the relative changes in $B\rho$ and C satisfy the following equation:

$$\frac{\mathrm{d}(B\rho)}{B\rho} = \gamma_t^2 \frac{\mathrm{d}C}{C}, \tag{3}$$

where the parameter γ_t serves as a bridge connecting the relative variations in $B\rho$ and C. Although γ_t is often considered constant with respect to C, it actually varies with C, forming a $\gamma_t(C)$ curve [29].

For simplicity, consider two ions simultaneously stored in the ring: One is a reference ion with a known mass, and the other is a non-reference ion with an unknown mass. Let $B\rho_0$ and C_0 represent the magnetic rigidity and orbit length of the reference ion, respectively, and $B\rho_x$ and C_x denote those of the non-reference ion. Note that $B\rho_0$, C_0, and C_x can be determined by measuring T and v for both ions. According to Eq. (3), one has:

$$\int_{B\rho_0}^{B\rho_x} \frac{\mathrm{d}(B\rho)}{B\rho} = \int_{C_0}^{C_x} \gamma_t^2(C)\frac{\mathrm{d}C}{C}. \tag{4}$$

By defining

$$K = \int_{C_0}^{C_x} \gamma_t^2(C)\frac{\mathrm{d}C}{C}, \tag{5}$$

which can be calculated through numerical integration as long as $\gamma_t(C)$ is known (details will be introduced later), $B\rho_x$ can be derived as:

$$B\rho_x = B\rho_0 \cdot e^K. \tag{6}$$

Through Eq. (6), $B\rho_x$ of the non-reference ion is obtained via a single reference ion in the same injection, and the mass value is directly determined via Eq. (2). Consequently, the effect of magnetic field drift between injections is expected to be effectively eliminated.

3 The γ_t, $B\rho$, and mass determination

Several methods have been developed to measure the γ_t values [28, 30], and their results are in excellent agreement. In this work, we employed the method using energy loss to calculate the $\gamma_t(C)$ values, owing to its simplicity. Details of this method can be found in Ref. [28].

Figure 1 illustrates a scatter plot of γ_t values obtained from all ions measured in the experiment using $^{58}Ni^{19+}$ as the primary beam [21, 23]. The unreasonable scattered points are primarily attributed to the low detection efficiency of the TOF detector for light ions [28]. To obtain more accurate averaged γ_t values, only ions with mass number A greater than 18 were adopted. The averaged γ_t values within approximately 3 -mm intervals are presented as red curves. The γ_t value at any C within the specified range can be determined using linear interpolation.

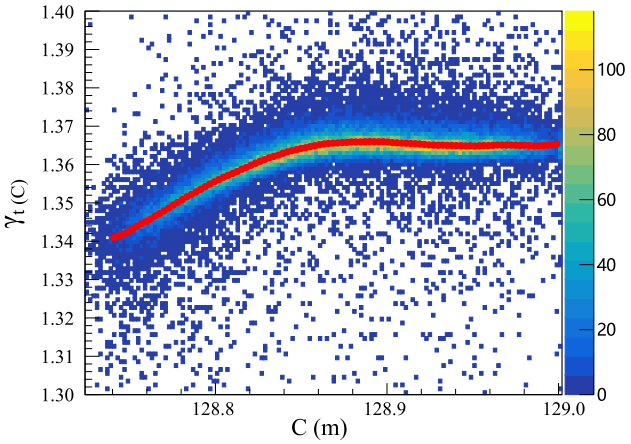

Fig. 1 (Color online) $\gamma_t(C)$ values obtained from all the measured ions in the experiment using $^{58}Ni^{19+}$ as primary beam. The red line represents the averaged $\gamma_t(C)$ values within a small orbit interval of approximately 3 mm

Using the $\gamma_t(C)$ curve, the parameter K defined in Eq. (5) is obtained through the following numerical integration:

$$K = \int_{C_0}^{C_x} \gamma_t^2(C)\frac{dC}{C} = \sum_{i=1}^{n} \gamma_t^2(C_i)\frac{\Delta C_s}{C_i}. \quad (7)$$

Here, $C_i = C_0 + i\Delta C_s$ and $\Delta C_s = (C_x - C_0)/n$, where n represents the number of intervals. By choosing a large n, or equivalently, a sufficiently small ΔC_s (e.g., 0.3 mm), the $\gamma_t(C)$ value within each interval can be regarded as constant during integration.

With the calculated K value, $B\rho_x$ was determined according to Eq. (6) based on the $B\rho_0$ value of the reference ion. If there are multiple reference ions in the same injection, the same number of $B\rho_x$ values will be obtained. All these $B\rho_x$ values were averaged to obtain the mean $B\rho_x$ value. Then, the m/q value is obtained using Eq. (2).

In this study, ions with mass uncertainties below 50 keV were selected as references to determine the mass values of non-reference ions. However, to validate the mass determination, the mass of each reference ion is first assumed to be unknown and then re-determined using the other reference ions in the same injection. As shown in Fig. 2, all the obtained m/q values were combined to form distinct m/q peaks.

Figure 3 compares the standard deviation $\sigma_{(m/q)}$ of m/q peaks (in units of keV/e) from three methods: this work, previous $B\rho$-IMS, and transformed from the original T peaks without any post-process procedure, such as the magnetic field correction procedure. Here, the transformed m/q peaks were obtained using Eq. (2), where $v = C/T$, and $B\rho$

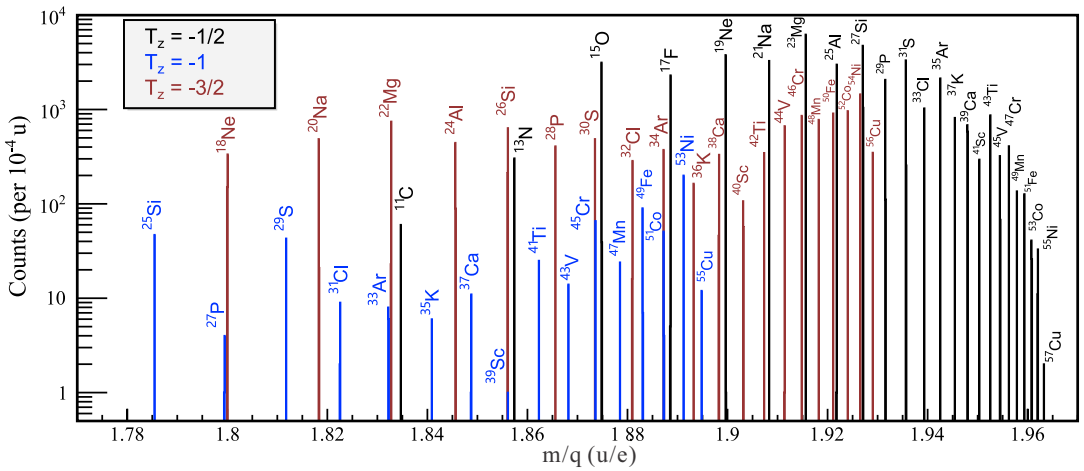

Fig. 2 (Color online) The m/q peaks obtained from this work. Different colors represent the series of nuclides with a constant isospin projection $T_z = (N - Z)/2$, as shown in the legend

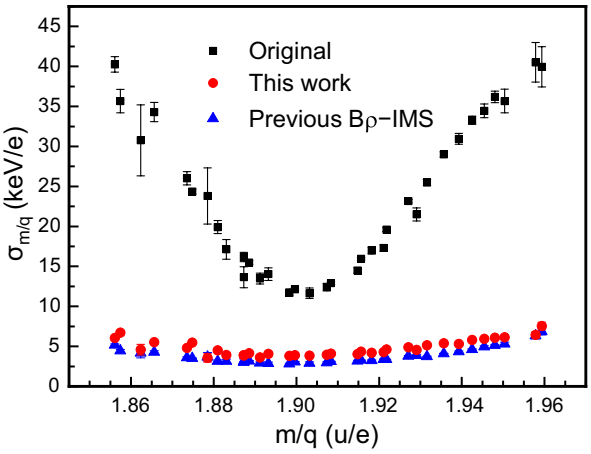

Fig. 3 (Color online) Standard deviations of the m/q peaks derived from the original T measurement (black squares), the previous $B\rho$-IMS method (blue triangles), and this work (red dots)

and C are fixed at 5.4758 T·m and 128.86 m, respectively (see Ref. [23] for more details). It can be observed that the $\sigma_{m/q}$ from this work is significantly lower than that transformed from the original T peaks but is comparable to those obtained from the previous $B\rho$-IMS. This indicates that the impact of magnetic field drifts on mass determination has been effectively eliminated by this new method. We note that this was achieved without any additional magnetic field correction procedures. Nevertheless, the $\sigma_{m/q}$ obtained in this study is slightly (approximately 1 keV/e) larger than that obtained from the previous $B\rho$-IMS results. This may be attributed to the variation of the $\gamma_t(C)$ curve caused by the magnetic field drifts during the experiment. Further discussion is provided in Sect. 4.

Assuming that each m/q value contributes equally, the final determined m/q and its uncertainty were calculated as follows:

$$\begin{aligned}\langle m/q\rangle &= \frac{\sum_{j=1}^{N}(m/q)_j}{N}\\ \sigma_{\langle m/q\rangle} &= \frac{\sigma_{m/q}}{\sqrt{N-1}},\end{aligned} \tag{8}$$

where N is the number of counts.

For each nuclide, the comparison of the mass excess (ME) with the literature value (e.g., the previous $B\rho$-IMS result [23]) is illustrated in Fig. 4, showing a good agreement between them.

To further quantitatively evaluate the agreement, the normalized χ_n defined as

$$\chi_n = \sqrt{\frac{1}{N_c}\sum_{i=1}^{N_c}\frac{(\mathrm{ME}^i_{\mathrm{exp}} - \mathrm{ME}^i_{\mathrm{lit}})^2}{\sigma^2_{\mathrm{exp}} + \sigma^2_{\mathrm{lit}}}} \tag{9}$$

is employed. Here, N_c is the total number of nuclides for comparison, $\mathrm{ME}^i_{\mathrm{exp}}$ and $\mathrm{ME}^i_{\mathrm{lit}}$ are the mass excesses determined in this study and from the literature, respectively, and σ_{exp} and σ_{lit} represent the corresponding mass uncertainties.

The obtained χ_n values of 0.80 and 0.53 for the reference and non-reference nuclides, respectively, indicate that the mass results from the two methods are in good agreement. However, the mass uncertainties in this study are slightly larger than those from the previous $B\rho$-IMS work, consistent with the slightly larger $\sigma_{m/q}$ observed in this study, as shown in Fig. 3.

We note that the two parameters L and Δt_d (see Ref. [23] for details) used to determine the velocity of each ion were optimized to minimize the χ^2 value. The literature ME values used for this optimization were taken from Ref. [31]. The obtained optimal values of $L = 18.046$ m and $\Delta t_d = -147.0$ ps agree well with those ($L = 18.046$ m and $\Delta t_d = -146.83$ ps) from the previous $B\rho$-IMS study [23].

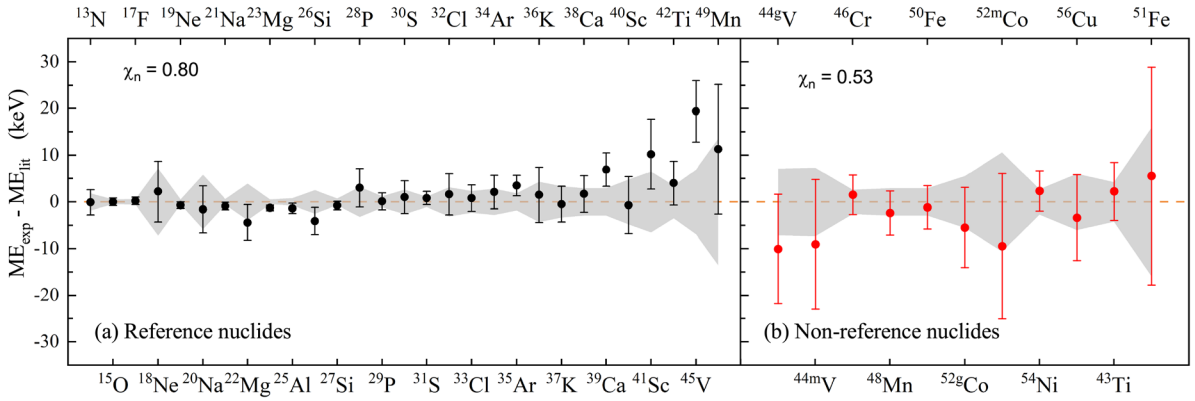

Fig. 4 The mass excess (ME) difference between this work and previous $B\rho$-IMS result of the same experiment [21, 23], for the reference (**a**) and non-reference nuclides (**b**). The demonstrated error bars are from this study, whereas the shaded areas represent the error bars from the previous $B\rho$-IMS ME results

4 Discussion

4.1 Effects of magnetic field (or γ_t) drifts

According to the study presented in Ref. [29], the $\gamma_t(C)$ curve is affected by magnetic field drifts. For example, it can be shifted horizontally, vertically, or rotated by varying the dipole, quadrupole, and sextupole magnetic fields. Given that the utilized $\gamma_t(C)$ value in this method is an average value over the entire experiment [28, 30], for each injection, the $\gamma_t(C)$ value may vary from this average value owing to magnetic field drifts, introducing potential uncertainties in the $B\rho$ and mass determination.

To quantitatively evaluate the effect of γ_t variation, we first assume that γ_t is independent of C. Considering that $\Delta C = C_x - C_0$ is much smaller than C_x or C_0, the parameter K can be approximated as:

$$K = \int_{C_0}^{C_x} \gamma_t^2(C)\frac{dC}{C} \simeq \gamma_t^2 \frac{\Delta C}{C_0}. \tag{10}$$

Because γ_t is close to one, the K value is on the same order of magnitude as $\Delta C/C_0$, which is significantly less than one. Consequently, according to Eq. (6), $B\rho_x$ can be estimated as:

$$B\rho_x \simeq B\rho_0 \cdot (1+K) \simeq B\rho_0 \cdot \left(1 + \gamma_t^2 \frac{\Delta C}{C_0}\right). \tag{11}$$

Assuming that the magnetic field drift induces a variation $\delta\gamma_t$ in γ_t, the corresponding variation in the calculated $B\rho_x$ is denoted as $\delta(B\rho_x)$. From Eq.(11), we obtain:

$$\frac{\delta(B\rho_x)}{B\rho_x} \simeq \frac{\delta(B\rho_x)}{B\rho_0} \simeq 2\gamma_t \cdot \frac{\Delta C}{C_0} \cdot \delta\gamma_t. \tag{12}$$

Combining Eq. (2) and Eq. (12), one yields:

$$\frac{\delta(m/q)}{m/q} \simeq \frac{\delta(B\rho_x)}{B\rho_x} \simeq 2\gamma_t^2 \cdot \frac{\Delta C}{C_0} \cdot \frac{\delta\gamma_t}{\gamma_t}. \tag{13}$$

Equation (13) clearly indicates that the effect of γ_t variation on the final mass value is significantly reduced by the small factor $\Delta C/C_0$, which is generally on the order of 10^{-4} in $B\rho$-IMS. In this experiment, the average $\Delta C/C$ ratio was approximately $\simeq 5\times10^{-4}$.

To further support this conclusion, we present a specific example from the ^{58}Ni experiment. The variation in the (dipole) magnetic fields with respect to the injection numbers is illustrated in Fig. 5a (one injection every 25 s; see Fig. 7a and the accompanying text in Ref. [23] for further details).

First, to examine the effect of magnetic field drifts on the $\gamma_t(C)$ curve, two injection groups marked in red and blue in Fig. 5a were selected. The corresponding $\gamma_t(C)$ curves are depicted in Fig. 5b, demonstrating horizontal shifts between the two groups, which is consistent with the conclusion drawn from Ref. [29]. The largest relative deviation occurred at the left part of the curve and reached approximately 10^{-3}.

Second, to quantify the impact of such $\gamma_t(C)$ variation, we examined a simplified scenario in which all $\gamma_t(C)$ values were systematically decreased by 10^{-3}, corresponding to a downward shift of the $\gamma_t(C)$ curve (Fig. 1) by this amount. The resulting $\sigma_{m/q}$ values are represented by triangles in Fig. 5c. These values are significantly smaller than the original values (squares), but are still approximately 1 keV/e larger than the normal values (circles) obtained using the unshifted $\gamma_t(C)$ curve. Notably, this magnitude of increase matches the discrepancy observed between our normal results (this work) and previous $B\rho$-IMS results (see Fig. 3). This suggests that variations in the $\gamma_t(C)$ curve, caused by the (dipole) magnetic field drifts, may be responsible for the observed discrepancy in $\sigma_{m/q}$ between the two methods.

Equation (13) indicates that a 10^{-3} shift in the $\gamma_t(C)$ curve introduces a relative m/q uncertainty: $\frac{\delta(m/q)}{m/q} \simeq 2\gamma_t^2 \cdot \frac{\Delta C}{C_0} \cdot \frac{\delta\gamma_t}{\gamma_t} \simeq 2\times1.36^2\times(5\times10^{-4})\times10^{-3} \simeq 2\times10^{-6}$. This corresponds to an expected additional uncertainty of $\sim$ 4 keV/e in m/q, leading to an approximate 1 keV/e increase in $\sigma_{m/q}$. This estimation is in agreement with the observed 1 keV/e increase in $\sigma_{m/q}$ in Fig. 5c, thereby confirming the validity of Eq. (13).

Finally, to demonstrate the effect of the $\gamma_t(C)$ curve with and without the artificial shift on the final mass determination, the differences in the resulting ME values are presented in Fig. 5d. Most of these differences lie within a narrow range of ±5 keV (see the shaded area in Fig. 5d), supporting the robustness of this method.

4.2 The advantage of requiring only one reference ion in each injection

Currently, nuclides with well-known masses have been extended to the quite exotic region, characterized by short half-lives and very low production yields. When measuring the mass values of mass-unknown nuclides using the $B\rho$ -IMS technique, the number of stored ions per injection can be remarkably low.

Figure 6 presents an example of the number of stored ions per injection in a $B\rho$-IMS experiment using ^{36}Ar as the primary beam. In this experiment, the magnetic rigidity of the beam lines was optimized to maximize the transport efficiency for the extremely exotic ion of $^{22}Si^{14+}$. Consequently, the most frequently observed number of stored ions per injection was reduced to approximately three. Under such conditions, the previous $B\rho$-IMS method, which requires as many reference ions as possible for magnetic field correction, encounters significant challenges. One potential solution is to discard injections containing fewer than, for

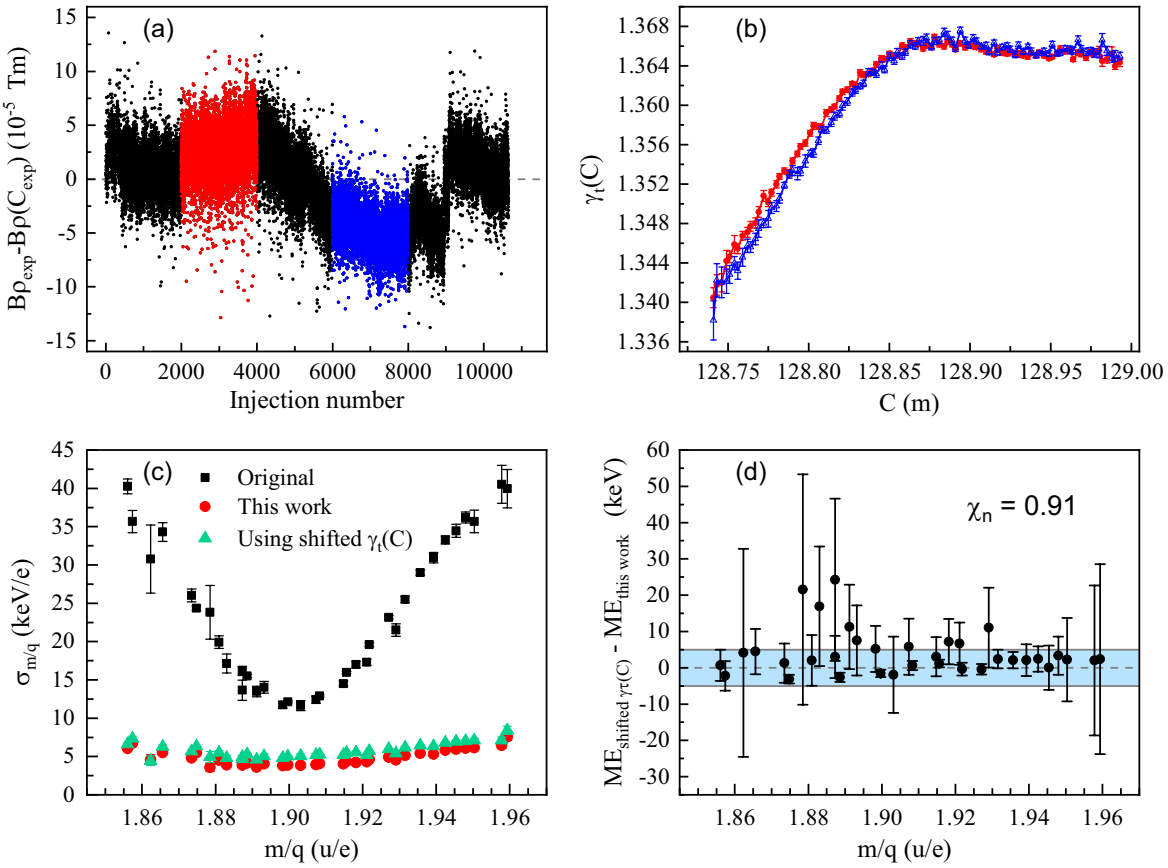

Fig. 5 (Color online) **(a)** The drifts of (dipole) magnetic field of CSRe as a function of injection number (see Fig. 7a in Ref. [23] for details). **(b)** The $\gamma_t(C)$ curve corresponding to the injections marked in **(a)** with red and blue colors, illustrating a horizontal shift caused by the magnetic field variation. The maximum relative change in the γ_t value at a certain C is on the order of 10^{-3}. **(c)** Similar to Fig. 3, but the green points represent the $\sigma_{m/q}$ values derived from the artificially downward-shifted $\gamma(C)$ curve in Fig. 1 by 10^{-3}. See the text for further details of the study. **(d)** The differences between the ME values resulting from the $\gamma_t(C)$ curve with and without the artificial shift. Most differences are within ±5 keV, as indicated by the shaded region

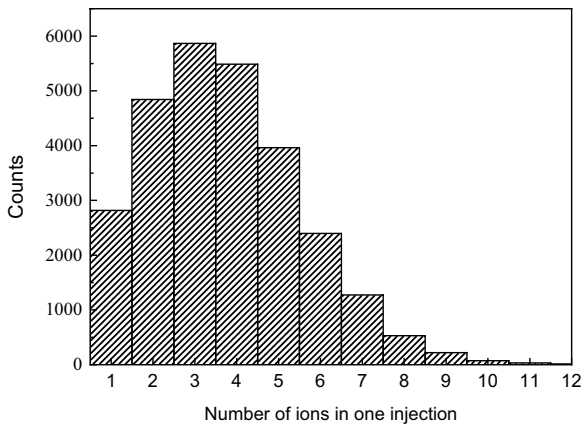

Fig. 6 The statistics of the numbers of ions per injection for the $B\rho$-IMS experiment using ^{36}Ar as primary beam, which aims to measure the mass value of very exotic nuclide ^{22}Si

example, three reference ions to ensure successful magnetic field correction. However, this approach leads to a significant loss of statistics (28%) and may introduce biases in the mass uncertainty assignments for both reference and non-reference ions. Alternatively, one could use the $B\rho$-C curve without magnetic field correction, but this would allow magnetic field fluctuations between injections to directly affect mass measurements at the 10^{-5} level, significantly degrading mass precision.

In such challenging scenarios, the method proposed in this study effectively overcomes all these challenges. It requires only one reference ion to determine unknown mass values and achieves high precision without the need for magnetic field correction. Using this method, the re-determined ME value of ^{23}Si, which is 23365(16) keV [32], is fully confirmed by the LEBIT Penning trap result of 23362.9(5.8) keV [33], demonstrating the efficiency and reliability of this important improvement for $B\rho$-IMS.

5 Summary and outlook

In this study, we propose a novel method relying on the $\gamma_t(C)$ curve for $B\rho$-IMS to determine nuclear mass values. This method significantly reduces the need to correct the effects of magnetic field drifts and requires only one reference ion with a known mass value for the mass determination of the ions of interest. Remarkably, the achieved mass precision without any correction procedure is still comparable to that of the previous $B\rho$-IMS method. Consequently, it not only simplifies the data analysis procedure for $B\rho$-IMS but is also suitable for future IMS experiments involving exotic nuclei with extremely low yields.

Nonetheless, further improvements to this method are possible. First, while this method significantly reduces the influence of variations in the $\gamma_t(C)$ curve (or magnetic field), residual effects cannot be entirely neglected, especially as the mass precision of $B\rho$-IMS is expected to continue improving. From this perspective, a more stable magnetic field environment remains essential. However, given that absolutely stable magnetic fields are technically unachievable, and considering that the drifts of the dipole magnetic field induce only a horizontal shift in the $\gamma_t(C)$ curve, a flatter $\gamma_t(C)$ curve would further minimize the impact of dipole magnetic field drifts on the final mass determinations and thus is highly desirable. Second, the current mass determination of this method relies on averaging all obtained m/q values under the assumption of equal contribution. Actually, each individual obtained m/q value has a different uncertainty, and the simple assumption may introduce deviations, particularly when the statistic is limited. Future refinements should incorporate uncertainty quantification for the individually obtained m/q values of each nuclide to enable a weighted mean value and uncertainty.

Author contributions All authors contributed to the study conception and design. Material preparation, data collection, and analysis were performed by Yin-Fang Luo, Jia-Hao Lv, Yuan-Ming Xing, and Min Zhang. The first draft of the manuscript was written by Yin-Fang Luo, and all authors commented on previous versions of the manuscript. All authors read and approved the final manuscript.

Data availability The data that support the findings of this study are openly available in Science Data Bank at https://cstr.cn/31253.11.sciencedb.35881 and https://www.doi.org/10.57760/sciencedb.35881.

Declarations

Conflict of interest The authors declare that they have no conflict of interest.

References

1. T. Yamaguchi, H. Koura, Y. Litvinov et al., Masses of exotic nuclei. Prog. Part. Nucl. Phys. **120**, 103882 (2021). https://doi.org/10.1016/j.ppnp.2021.103882
2. Y. Zhang, S.Q. Yan, M. He et al., Stepped-up development of accelerator mass spectrometry method for the detection of 60fe with the hi-13 tandem accelerator. Nucl. Sci. Tech. **35**, 77 (2024). https://doi.org/10.1007/s41365-024-01453-x
3. S. Jiang, M. He, K.J. Dong, *Accelerator Mass Spectrometry Techniques and Applications*, 1st edn. (Nuclear Science and Technology, Springer Singapore, 2025)
4. X.L. Tu, H.S. Xu, M. Wang et al., Direct mass measurements of short-lived $A = 2Z-1$ nuclides ^{63}Ge, ^{65}As, ^{67}Se, and ^{71}Kr and their impact on nucleosynthesis in the *rp* process. Phys. Rev. Lett. **106**, 112501 (2011). https://doi.org/10.1103/PhysRevLett.106.112501
5. Y.H. Zhang, H.S. Xu, Y.A. Litvinov et al., Mass measurements of the neutron-deficient ^{41}Ti, ^{45}Cr, ^{49}Fe, and ^{53}Ni nuclides: First test of the isobaric multiplet mass equation in *fp*-shell nuclei. Phys. Rev. Lett. **109**, 102501 (2012). https://doi.org/10.1103/PhysRevLett.109.102501
6. X. Xu, P. Zhang, P. Shuai et al., Identification of the lowest $T = 2$, $J^\pi = 0^+$ isobaric analog state in ^{52}Co and its impact on the understanding of β-decay properties of ^{52}Ni. Phys. Rev. Lett. **117**, 182503 (2016)
7. R. Knobel, M. Diwisch, F. Bosch et al., First direct mass measurements of stored neutron-rich ^{129,130,131}Cd isotopes with FRS-ESR. Phys. Lett. B **754**, 288–293 (2016). https://doi.org/10.1016/j.physletb.2016.01.039
8. Y.H. Zhang, P. Zhang, X.H. Zhou et al., Isochronous mass measurements of $T_z = -1$ *fp*-shell nuclei from projectile fragmentation of ^{58}Ni. Phys. Rev. C **98**, 014319 (2018). https://doi.org/10.1103/PhysRevC.98.014319
9. Y.M. Xing, K.A. Li, Y.H. Zhang et al., Mass measurements of neutron-deficient Y, Zr, and Nb isotopes and their impact on *rp* and *vp* nucleosynthesis processes. Phys. Lett. B **781**, 358–363 (2018). https://doi.org/10.1016/j.physletb.2018.04.009
10. Y.M. Xing, C.X. Yuan, M. Wang et al., Isochronous mass measurements of neutron-deficient nuclei from ^{112}Sn projectile fragmentation. Phys. Rev. C **107**, 014304 (2023). https://doi.org/10.1103/PhysRevC.107.014304
11. D. Lunney, New mass measurements with trapped (radioactive) ions and related fundamental physics. Hyperfine Interact. **240**, 48 (2019). https://doi.org/10.1007/s10751-019-1581-z
12. M. Steck, Y.A. Litvinov, Heavy-ion storage rings and their use in precision experiments with highly charged ions. Prog. Part. Nucl. Phys. **115**, 103811 (2020). https://doi.org/10.1016/j.ppnp.2020.103811
13. P.M. Walker, Double-up for single-ion masses. Nucl. Sci. Tech. **34**, 104 (2023). https://doi.org/10.1007/s41365-023-01250-y
14. M. Hausmann, F. Attallah, K. Beckert et al., First isochronous mass spectrometry at the experimental storage ring ESR. Nucl. Instrum. Methods Phys. Res., Sect. A Accel. Spect. Detect. Assoc. Equip. **446**, 569–580 (2000). https://doi.org/10.1016/S0168-9002(99)01192-4
15. H. Geissel, R. Knöbel, Y.A. Litvinov et al., A new experimental approach for isochronous mass measurements of short-lived exotic nuclei with the FRS-ESR facility. Hyperfine Interact. **173**, 49–54 (2006). https://doi.org/10.1007/s10751-007-9541-4
16. H.Y. Deng, Y.M. Xing, X. Zhou et al., Improved isochronous mass spectrometry with tune measurement. Nucl. Sci. Tech. **35**, 203 (2024). https://doi.org/10.1007/s41365-024-01580-5
17. J.H. Liu, Z. Ge, Q. Wang et al., Electrostatic-lenses position-sensitive TOF MCP detector for beam diagnostics and new scheme

for mass measurements at HIAF. Nucl. Sci. Tech. **30**, 152 (2019). https://doi.org/10.1007/s41365-019-0676-1
18. H. Geissel, Y.A. Litvinov, Precision experiments with relativistic exotic nuclei at GSI. J. Phys. G: Nucl. Part. Phys. **31**, S1779–S1783 (2005). https://doi.org/10.1088/0954-3899/31/10/072
19. Y.M. Xing, M. Wang, Y.H. Zhang et al., First isochronous mass measurements with two time-of-flight detectors at CSRe. Phys. Scr. **T166**, 014010 (2015). https://doi.org/10.1088/0031-8949/2015/t166/014010
20. X. Zhou, M. Zhang, M. Wang et al., In-ring velocity measurement for isochronous mass spectrometry. Phys. Rev. Accel. Beams **24**, 042802 (2021). https://doi.org/10.1103/PhysRevAccelBeams.24.042802
21. M. Wang, M. Zhang, X. Zhou et al., Bρ-defined isochronous mass spectrometry: An approach for high-precision mass measurements of short-lived nuclei. Phys. Rev. C **106**, L051301 (2022). https://doi.org/10.1103/PhysRevC.106.L051301
22. X. Zhou, M. Wang, Y.H. Zhang et al., Bρ-defined isochronous mass spectrometry at the storage ring CSRe. Nucl. Sci. Tech. **35**, 213 (2024). https://doi.org/10.1007/s41365-024-01587-y
23. M. Zhang, X. Zhou, M. Wang et al., $B\rho$-defined isochronous mass spectrometry and mass measurements of ^{58}Ni fragments. Eur. Phys. J. A **59**, 27 (2023). https://doi.org/10.1140/epja/s10050-023-00928-6
24. M. Wang, Y.H. Zhang, X. Zhou et al., Mass measurement of upper *fp*-shell $N = Z - 2$ and $N = Z - 1$ nuclei and the importance of three-nucleon force along the $N = Z$ line. Phys. Rev. Lett. **130**, 192501 (2023). https://doi.org/10.1103/PhysRevLett.130.192501
25. Y. Yu, Y.M. Xing, Y.H. Zhang et al., Nuclear structure of dripline nuclei elucidated through precision mass measurements of ^{23}Si, ^{26}P, ^{27,28}S, and ^{31}Ar. Phys. Rev. Lett. **133**, 222501 (2024). https://doi.org/10.1103/PhysRevLett.133.222501
26. X. Zhou, M. Wang, Y.H. Zhang et al., Mass measurements show slowdown of rapid proton capture process at waiting-point nucleus ^{64}Ge. Nature Physics **19**, 1091–1097 (2024). https://doi.org/10.1038/s41567-023-02034-2
27. Y.M. Xing, Y.H. Zhang, M. Wang et al., Particle identification and revolution time corrections for the isochronous mass spectrometry in storage rings. Nucl. Instrum. Methods Phys. Res. Sect. A Accel. Spectromet. Detect. Assoc. Equip. **941**, 162331 (2019). https://doi.org/10.1016/j.nima.2019.06.072
28. M. Zhang, Y. Zhang, M. Wang et al., Precision measurement of the transition energy γ_t versus magnetic rigidity for storage-ring isochronous mass spectrometry. Nucl. Instrum. Methods Phys. Res. Sect. A Accel. Spectromet. Detect. Assoc. Equip **1027**, 166329 (2022). https://doi.org/10.1016/j.nima.2022.166329
29. W. W. Ge, Y. J. Yuan, J. C. Yang, et al., Experimental investigation of the transition energy γ_t in the isochronous mode of the HIRFL-CSRe. Nucl. Instrum. Methods Phys. Res. Sect. A Accel. Spectromet. Detect. Associat. Equip. 908, 388–393 (2018). https://doi.org/10.1016/j.nima.2018.08.059
30. R.J. Chen, X.L. Yan, W.W. Ge et al., A method to measure the transition energy γ_t of the isochronously tuned storage ring. Nucl. Instrum. Methods Phys. Res. Sect. A Accel. Spectromet. Detect. Assoc. Equip. **898**, 111–116 (2018). https://doi.org/10.1016/j.nima.2018.04.056
31. M. Wang, W.J. Huang, F.G. Kondev, et al., The AME 2020 atomic mass evaluation (II). tables, graphs and references*. Chinese Phys. C 45, 030003 (2021). https://doi.org/10.1088/1674-1137/abddaf
32. Y.M. Xing, Y.F. Luo, Y.H. Zhang et al., $Z = 14$ magicity revealed by the mass of the proton dripline nucleus ^{22}Si. Phys. Rev. Lett. **135**, 012501 (2025). https://doi.org/10.1103/ffwt-n7yc
33. F.M. Maier, G. Bollen, B.A. Brown et al., Exploring isospin symmetry breaking in exotic nuclei: High-precision mass measurement of ^{23}Si and shell-model calculations of $T = 5/2$ isotopes. Phys. Rev. C **112**, 014329 (2025). https://doi.org/10.1103/14s5-17gj